ELSEVIER

Journal of Hazardous Materials 74 (2000) 1–23

Journal of Hazardous Materials

www.elsevier.nl/locate/jhazmat

Speciation of elements in NIST particulate matter SRMs 1648 and 1650

Frank E. Huggins [a,*], Gerald P. Huffman [a], J. David Robertson [b]

[a] *Department of Chemical and Materials Engineering, University of Kentucky, Lexington, KY 40506, USA*
[b] *Department of Chemistry, University of Kentucky, Lexington, KY 40506, USA*

Abstract

X-ray absorption fine structure (XAFS) spectra for S, Cl, V, Cr, Mn, Cu, Zn, As, Br, Cd and Pb and Mössbauer spectra for Fe have been obtained for two National Institute of Standards and Technology (NIST) particulate matter (PM) standard reference materials (SRMs): urban PM (SRM 1648) and diesel PM (SRM 1650). The spectral data, complemented by information on elemental concentrations from proton-induced X-ray-emission (PIXE) spectroscopy, were used to interpret the speciation of these elements in these complex materials. It appears that all the metallic elements investigated occur in oxidized forms, principally as sulfates in the diesel PM SRM and as sulfates, oxides, and possibly other forms (e.g. clays?) in the urban PM. A minor fraction of the sulfur and major fractions of the halogens, Cl and Br, occur as organosulfide (thiophene) and organohalide occurrences, respectively, that must be associated with the abundant carbonaceous matter that constitutes the major component of the two PM SRMs. Most of the sulfur, however, occurs as sulfate in the urban PM and as bisulfate in the diesel PM. In addition, elemental oxidation states have been determined directly by the spectroscopic techniques. Such information is often the key parameter in determining the toxicity and solubility of specific elements in PM, both of which are important in understanding the threat that such elements may pose to human health. For the two HAP elements, Cr and As, for which the toxicity depends greatly on oxidation state, the XAFS data showed that both elements are present in both SRMs predominantly in the less toxic oxidation states, Cr(III) and As(V). The potential of the XAFS spectra for use as source apportionment signatures is illustrated by reference to chromium, which exists in these two PM SRMs in very different forms.

Keywords: Particulate matter; Element speciation; XAFS spectroscopy; Standard reference materials; Oxidation state

* Corresponding author. 533 S. Limestone St., Suite 111, University of Kentucky, Lexington, KY 40506-0043, USA. Tel.: +1-606-257-4045; fax: +1-606-257-7215.

E-mail address: fhuggins@engr.uky.edu (F.E. Huggins).

0304-3894/00/$ - see front matter
PII: S0304-3894(99)00195-8

1. Introduction

Respirable fractions of airborne ambient particulate matter (PM), specifically those fractions that are less than 10 μm (PM_{10}) and more recently, less than 2.5 μm ($PM_{2.5}$) in size, have been identified as potential health concerns for the general public [1]. Much of this airborne PM is thought to derive from fossil fuel combustion, either from stationary sources such as coal or oil combustion plants for electrical-power generation or from vehicular exhausts, particularly diesel engines. The recently revised air quality standards proposed for ambient PM [1] have stimulated much new research on the health and environmental problems posed by such fine airborne material [2,3]. However, the actual deleterious agents in PM that adversely affect human health have not yet been identified. What appears to be of greatest concern are potentially toxic species that can dissolve in lung fluids and enter the body via the bloodstream. Such toxic species may either be organic or inorganic in origin.

Furthermore, owing to the chemical complexity, extremely small particle sizes, and the typically small total sample size (often no more than a few milligrams) of ambient PM samples collected on filters, such samples can pose significant problems for analysis, especially for speciation of the inorganics. One technique that has a significant potential for elemental speciation of fine PM is the synchrotron-based technique of X-ray absorption fine structure (XAFS) spectroscopy. This technique provides information on the form of occurrence of an element in the material under investigation, which complements compositional elemental analyses obtained by conventional methods, such as X-ray fluorescence, instrumental neutron activation analysis, proton-induced X-ray-emission (PIXE), etc. In addition, the XAFS technique is non-destructive, sensitive to parts-per-million (ppm) concentration levels of many elements, and is well suited for use directly with either bulk samples or PM filter samples.

A second aspect of the analysis of fine airborne ambient PM to which XAFS spectroscopy may contribute significantly is source apportionment. Source apportionment is likely to be an important issue in determining the relative responsibility (and hence, also to indicate the means for reducing airborne PM) of various anthropogenic contributions to the degradation of ambient air quality. Of particular concern is the recognition and measurement of different contributions, both natural and anthropogenic, to fine PM in ambient air. The spectral signatures obtained by XAFS spectroscopy for key elements could find use for recognizing specific individual source contributions to PM samples. However, the database on XAFS spectra of elements in both ambient PM samples and potential emission sources of PM will need to be generated, as there is very limited data available at this time.

In this paper, we summarize speciation data obtained from XAFS spectroscopy for various elements and from Mössbauer spectroscopy for iron in two National Institute of Standards and Technology (NIST) standard reference materials (SRMs) for PM: SRM 1648 Urban PM and SRM 1650 Diesel PM. Complementary analytical data from PIXE analyses are also summarized for the two SRMs. The emphasis is placed on those elements that are either transition metals or elements defined as hazardous air pollutants in the 1990 Amendments to the Clean Air Act [4]. A comparison of the XAFS and PIXE

data shown here for the bulk SRM samples with data obtained for a PM_{10} filter sample is to be presented elsewhere [5].

2. Experimental

2.1. XAFS spectroscopy

XAFS spectroscopy for S and Cl was performed at beam-line X-19A at the National Synchrotron Light Source (NSLS), Brookhaven National Laboratory, NY, using silicon (111) monochromator crystals, whereas the XAFS spectra for all other elements, V, Cr, Mn, Cu, Zn, As, Br, Cd, and Pb, were measured at beam-line IV-3 at the Stanford Synchrotron Radiation Laboratory (SSRL), Stanford University, CA, using silicon (220) monochromator crystals. All spectra were collected in fluorescence geometry using either a Lytle detector [6] or a 13-element germanium detector [7]. To enhance the signal/noise ratio, each Ge detector element was electronically gated to record just the X-rays fluoresced by the element of interest in response to the absorption of the incident X-rays. Typically, the XAFS data were collected from 100 eV below the absorption edge of the element of interest to as much as 500 eV above the edge. Where possible, each spectrum was calibrated simultaneously using a metal foil or other standard absorber in an absorption geometry experiment located after the fluorescence experiment. Also, filters and Soller slits [8] were used as needed to enhance the signal/noise ratio. Specific details of the XAFS experimentation are summarized in Table 1.

All spectra were obtained from samples of the urban and diesel SRMs held in the X-ray beam in thin polypropylene bags. Except for some minimal sample pulverization

Table 1
Details of XAFS experimentation for each element

Element[a]	Calibration material[b]	Calibration energy (eV)[c]	Detection method	Filter and other comments
S	Elem. S (peak)	2472	Lytle	None, all He path
Cl	NaCl	2825	Lytle	None, all He path
V	V foil	5465	13-Ge	3 μ Ti
Cr	Cr foil	5989	13-Ge	3 μ V
Mn	Mn foil	6539	13-Ge	6 μ Cr
Cu	Cu foil	8979	13-Ge	6 μ Ni
Zn	Zn foil	9659	13-Ge	6 μ Cu
As	As_2O_3 (peak)	11,867	13-Ge	6 μ Ge
Br	KBr	13,474	13-Ge	6 μ Se
Cd	Cd foil	26,711	13-Ge	None
Pb L_{III}	Pb foil	13,055	13-Ge	6 μm Ge

[a]All elements measured at their K-edge except for lead.

[b]All calibration points are the first inflection point in the XANES spectrum of the appropriate calibration material, except for sulfur and arsenic, in which cases the actual position of the prominent white-line peak of the calibration material was used.

[c]This energy is also the actual energy of the zero-points of energy for the compilations of XANES spectra shown in various figures in this paper.

and mixing in a mortar, nothing was done to the samples before placing them in the bags.

The XAFS spectral data were transferred electronically to a DEC MicroVAX computer workstation at the University of Kentucky for data analysis and reduction. The XAFS data reduction followed well-described standard procedures [9–11]. First, the raw spectrum was divided into separate X-ray absorption near-edge structure (XANES) and extended X-ray absorption fine structure (EXAFS) regions. Whereas the XANES region is used without further manipulation as a ''fingerprint'' for the occurrence of the element in the SRM, the EXAFS region is first converted to a reciprocal space representation and then subjected to a Fourier transform to obtain a ''radial structure function'' (RSF). The RSF is a one-dimensional representation of the local atomic structure that surrounds the absorbing atom. Either the XANES or the RSF, or both, can be used to infer how an element occurs in the material under investigation. However, due to reasons of either an insufficiently high concentration of the element or an insufficient range of energy for the EXAFS region as a consequence of the presence of absorption edges of other elements (e.g. V, see below), the RSFs were not always available or of useful quality.

2.2. Mössbauer spectroscopy

The speciation of iron in the urban PM sample was investigated using ^{57}Fe Mössbauer spectroscopy, a technique that is superior for determining iron speciation than iron XAFS spectroscopy. The Mössbauer spectrometer consisted of a control unit and constant acceleration driving unit supplied by Halder Electronik, that was interfaced to an MS-DOS 286DX personal computer via MCA/PHA boards from Canberra Nuclear. Spectra of both the unknown sample and a thin metallic iron foil for energy-scale calibration were collected simultaneously from separate ^{57}Co(Pd) sources attached to opposite ends of the drive. The spectra were obtained over a period of about 48 h in symmetric mode in acquisition groups of 1024 channels and a channel dwell-time of 100 μs. The spectra were transferred to an archival MicroVAX work-station for data storage and then subjected to analysis using a computerized least-squares fitting routine, described in detail elsewhere [12]. This routine fits Mössbauer spectra as a combination of one-line, two-line (quadrupole doublets) and six-line (magnetic hyperfine sextets) absorption units, each of which can be attributed to a specific iron species. The individual lines are assumed to be of Lorentzian shape. The distribution of iron among the different species recognized in the Mössbauer spectrum was based on the relative areas of the individual absorption units contributing to the overall spectrum [12]. Sample preparation for Mössbauer spectroscopy involved minor pulverization and mixing of the SRM in a mortar and pestle, followed by suspension of about 500 mg in the γ-ray beam by means of a 1.5-cm diameter, thin-walled plastic holder that presents a circular, thin aspect to the beam.

2.3. PIXE analysis

Non-destructive thick target PIXE analyses were performed on the SRM samples using the dual-energy irradiation procedure [13]. Protons with energies of 1.6 and 2.1

MeV, generated in a tandetron made by General Ionex, were used as the excitation source. Data analysis was performed using a modified version of the GUPIX PC-based software package [14]. The SRM samples were pressed into coherent pellets using a minimum of binder before being suspended in the particle beam.

2.4. Samples

NIST SRM 1648 urban PM [15] was collected in the St. Louis, MO, area over a 12-month period. It was collected in a bag-house designed especially for the purpose. The collected particulate material was removed from the filter bags, combined into a single lot, screened through a fine-mesh sieve to remove extraneous materials, thoroughly blended in a V-blender, and then packaged into bottles. Testing on at least six randomly selected bottles indicated no significant variation in analysis.

NIST SRM 1650 diesel PM [16] was collected from the heat-exchangers of a dilution tube facility following 200 engine hours of particle accumulation from several direct injection four-cycle diesel engines operating under a variety of conditions. It is considered to be representative of heavy-duty diesel engine particulate emissions.

A variety of additional analytical data is summarized for both SRMs in their respective NIST certificates of analysis [15,16].

Table 2
Element concentrations in NIST SRM particulate samples by PIXE analysis (in ppm, except where indicated as %, for wt.%)

Element by PIXE analysis	Urban particulate (NIST SRM 1648)	Diesel particulate (NIST SRM 1650)
C + (H, O, N, etc.)	> 70%	> 98%
Na	5000	< dl
Mg	5300	< dl
Al	2.33%	< dl
Si	7.92%	160
P	7700	740
S	4.55%	1.45%
Cl	4000	120
K	8300	< dl
Ca	5.52%	2300
Ti	3500	< dl
V	< dl	< dl
Cr	320	62
Mn	680	15
Fe	3.29%	690
Ni	57	50
Cu	514	50
Zn	4130	870
As	< dl	3.0
Br	430	3.5
Sr	220	< dl
Cd	< dl	< dl
Pb	6720	23

< dl — Below detection limit.

3. Results and discussion

3.1. PIXE spectroscopy

The PIXE analyses of the NIST SRMs are summarized in Table 2. More than 70 and 98 wt.% of the urban PM and diesel PM samples, respectively, are carbonaceous; that is, they consist of carbon, oxygen, nitrogen and perhaps other elements that commonly constitute organic matter. Sulfur is the dominant non-organic element in the diesel PM, while the analysis of the urban PM indicates the presence of significant quantities of aluminosilicates, possibly a K-bearing illitic clay, as well as various sulfur, iron, and calcium phases. A wide range of minor and trace elements occurs in the urban PM;

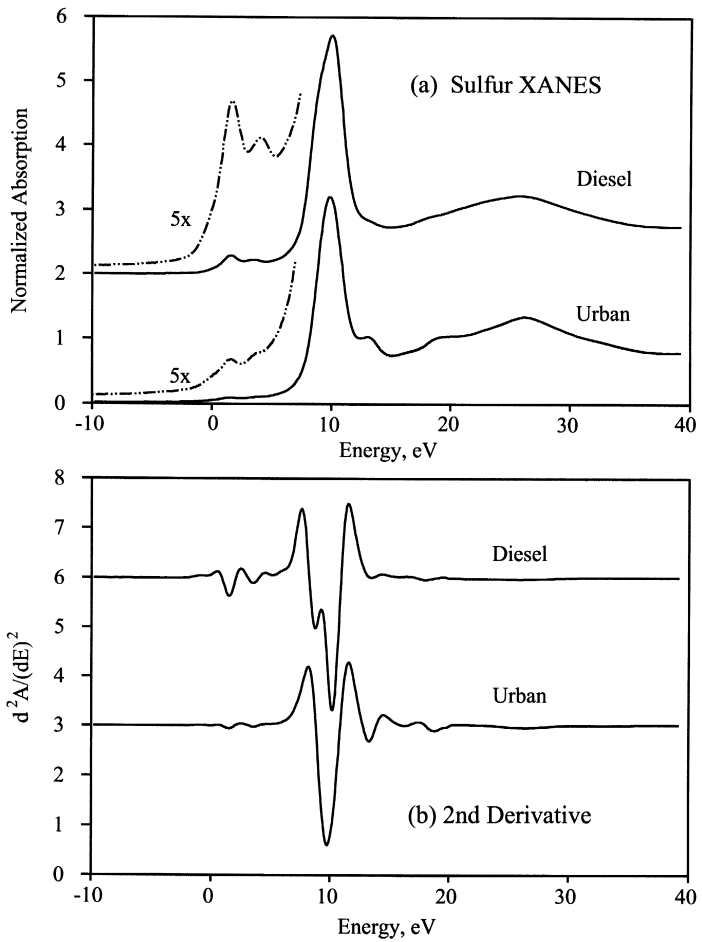

Fig. 1. (a) Sulfur XANES spectra of the NIST urban and diesel PM SRMs. Note the presence of organosulfur forms (small peaks, exaggerated by five times at about 1–2 eV) in addition to the dominant sulfate peaks at about 10 eV. (b) Second derivative spectra of the sulfur XANES spectra shown in Fig. 2(a). Note the asymmetry in the derivative spectrum of the diesel PM, indicating the presence of bisulfate.

whereas, the significant trace elements in the diesel PM sample include only Zn, P, Cl, Cr, Fe, and possibly Cu and Pb.

3.2. XAFS and ^{57}Fe Mössbauer data

XAFS data have been collected for S, Cl, V, Cr, Mn, Cu, Zn, As, Br, Cd, and Pb, in the urban and diesel PM SRMs. Each of these elements will be discussed individually. Also included in this section are speciation data for iron in the urban PM based on ^{57}Fe Mössbauer data.

3.2.1. Sulfur

As shown in Fig. 1, XANES spectra were obtained for both SRM samples. Both spectra consist of a very strong peak near 10 eV and two much weaker peaks near 1.5 and 3.5 eV. Based on XANES systematics for many sulfur compounds [17,18], the

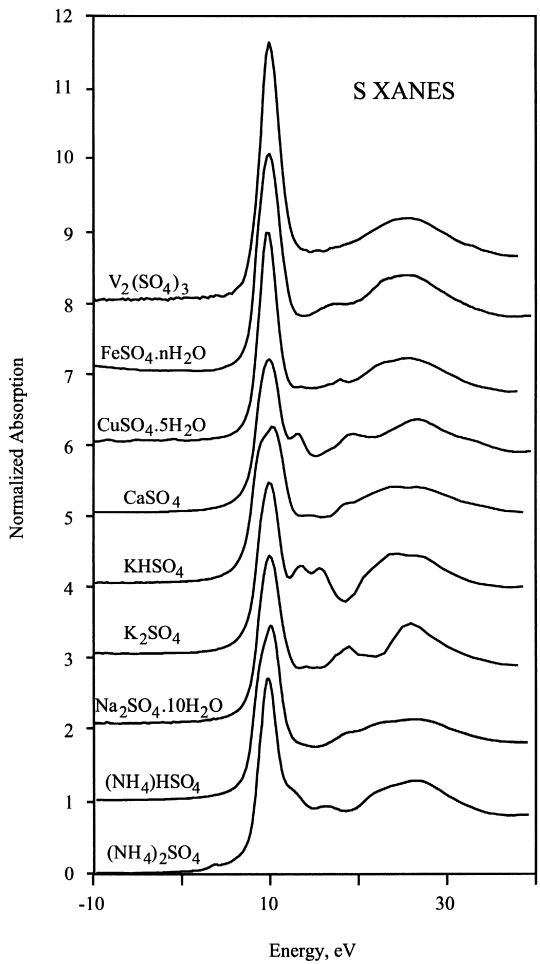

Fig. 2. Suite of sulfur XANES spectra for various sulfate and bisulfate standards.

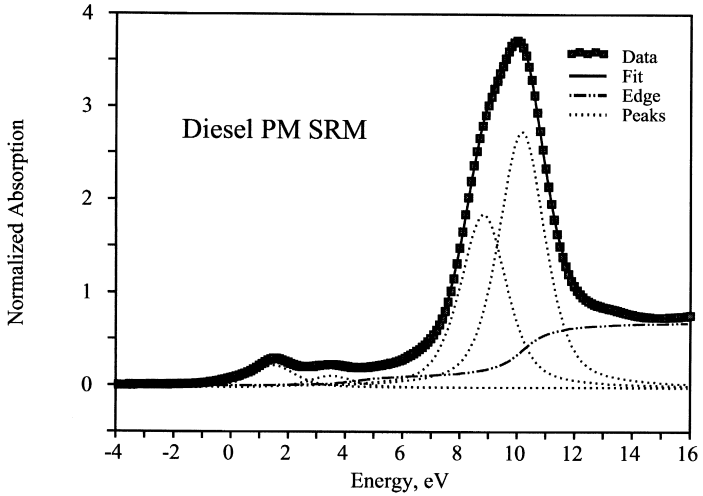

Fig. 3. Least-squares fitted sulfur XANES spectrum of the NIST diesel PM SRM, analyzed according to the method described elsewhere [18,19].

strong peak at 10 eV is identified as arising from sulfate. The shapes of the sulfate peaks differ significantly between the two samples; the peak for the diesel PM is asymmetric, as is reflected more clearly in the second derivative spectra (Fig. 1b). A similar asymmetry in peak shape is exhibited in Fig. 2 by the bisulfates of potassium and ammonium, when compared to the corresponding sulfate. Hence, whereas the peak at 10 eV for the urban PM reflects predominantly a sulfate (SO_4^{2-}) species, the asymmetric peak for the diesel PM reflects predominantly a bisulfate (HSO_4^-) species. Based on a comparison of the sulfur (S) XANES for the PM samples with those of the sulfate standards shown in Fig. 2, the urban PM appears to contain a significant fraction of $CaSO_4$. The weaker peaks at lower energy are consistent with thiophene or similar aromatic sulfur derivatives that are most likely associated with the abundant carbonaceous material in both samples.

A least-squares fitting procedure, developed for analyzing sulfur forms in coal and other fossil fuels [18,19], was used to estimate the relative proportions of sulfur forms in the PM samples. An example of the computerized fit to the data is given in Fig. 3 for the diesel PM, and the results of the analysis for both samples are summarized in Table 3.

Table 3
Results from least-squares fitting of sulfur XANES spectra

Sample	Thiophene (%S)	Sulfate (%S)	Bisulfate (%S)
Urban PM SRM 1648	2	90–98	<10
Diesel PM SRM 1650	10	0–30	60–90

Estimated experimental errors are $\pm 2\%$ for thiophene relative to the sulfate forms; however, the discrimination between sulfate and bisulfate has not been quantified and semi-quantitative estimates are given for these forms.

Both samples contain only minor but significant amounts of aromatic sulfur forms. The large uncertainty in the bisulfate determination is due to the lack of quantitative information available on the S XANES of such species.

3.2.2. Halogens

The XANES spectra of chlorine and bromine in the NIST SRMs are shown in Fig. 4a and b, respectively. The obvious difference in signal/noise ratio between the two samples for each element reflects the different concentrations of the elements in the two samples (Table 2). There are clear differences in the form of occurrence of chlorine in the two samples indicated by a comparison of the chlorine XANES spectra shown in Fig. 4a and those published in the literature [20]. The position of the first sharp peak, below 0 eV, and the subsequent close spacing of the broader peaks above 0 eV for the

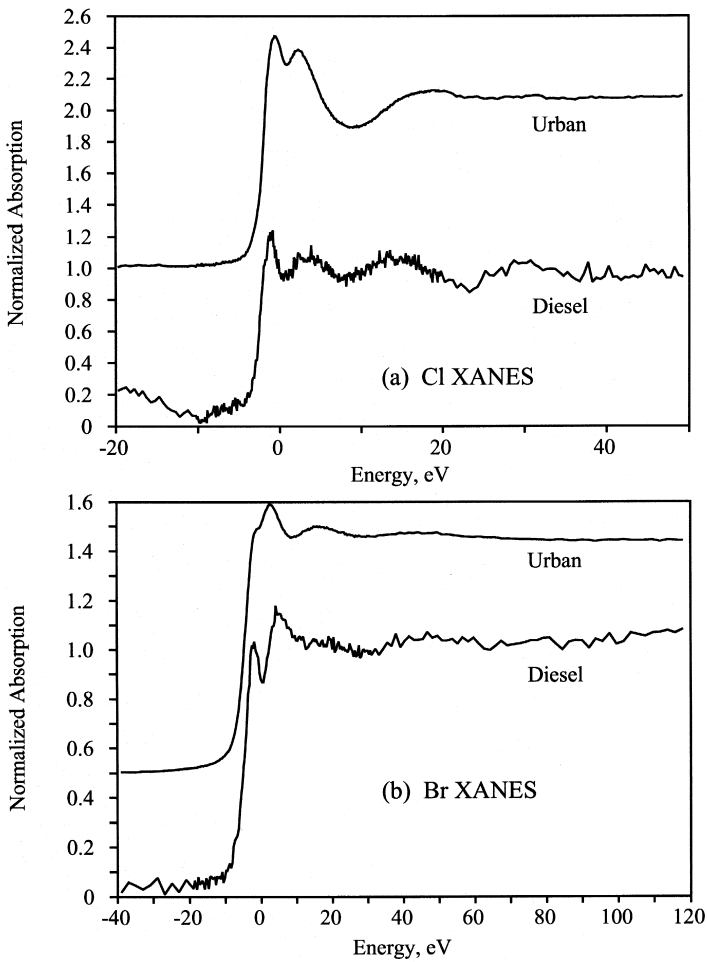

Fig. 4. (a) Chlorine XANES spectra of the NIST urban and diesel PM SRMs. (b) Bromine XANES spectra of the NIST urban and diesel PM SRMs.

diesel PM are consistent with chlorine predominantly in an organic phase; whereas, the spectrum for the urban PM appears to indicate an inorganic association for the chlorine, probably as chloride anions [20].

There are fewer data available for bromine, and the bromine XANES spectra of the SRMs (Fig. 4b) show less obvious differences than the chlorine spectra. However, as for Cl, there is a prominent sharp low-energy peak in the bromine XANES spectrum of the diesel PM that can be attributed to organobromine species and it can be concluded that organobromine compounds are more prevalent in the diesel PM than in the urban PM.

3.2.3. Vanadium

The vanadium XAFS spectrum was collected from both samples, however, the vanadium content of the diesel PM was too low to obtain a reasonable spectrum. The

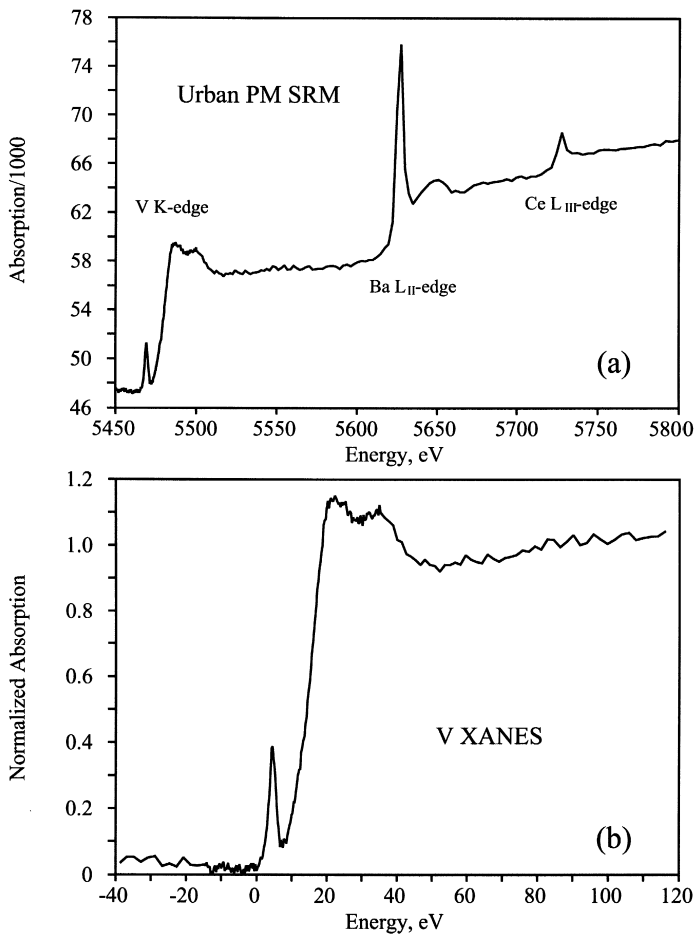

Fig. 5. (a) As-measured vanadium K-edge XAFS spectrum of the NIST urban PM SRM. Note the limited extent of the vanadium EXAFS region due to the presence of the prominent barium L_{II}-edge. (b) Vanadium XANES spectrum of the NIST urban PM SRM.

XAFS spectrum of the urban PM, shown in Fig. 5a, demonstrates a limitation of XAFS spectroscopy. In chemically complex materials, such as PM, in which many elements can be present, the EXAFS information available for a given element may be limited by the presence of a second element. In this particular case, the presence of a strong L_{II}-edge of barium limits the EXAFS region for vanadium to about 120 eV, which is too short a range of energy over which to obtain a useful RSF. However, the presence of barium does not affect the observation of the vanadium K-edge XANES region, and that information is still available for interpretation of the speciation of vanadium.

The vanadium XANES spectrum of the urban PM that is obtained by conventional manipulation of the XAFS spectrum is shown in Fig. 5b. It includes a pre-edge feature at 4.4 eV that is reasonably sharp and symmetric, suggesting that vanadium is predominantly in a single oxidation state. Based on the normalized height and position of the

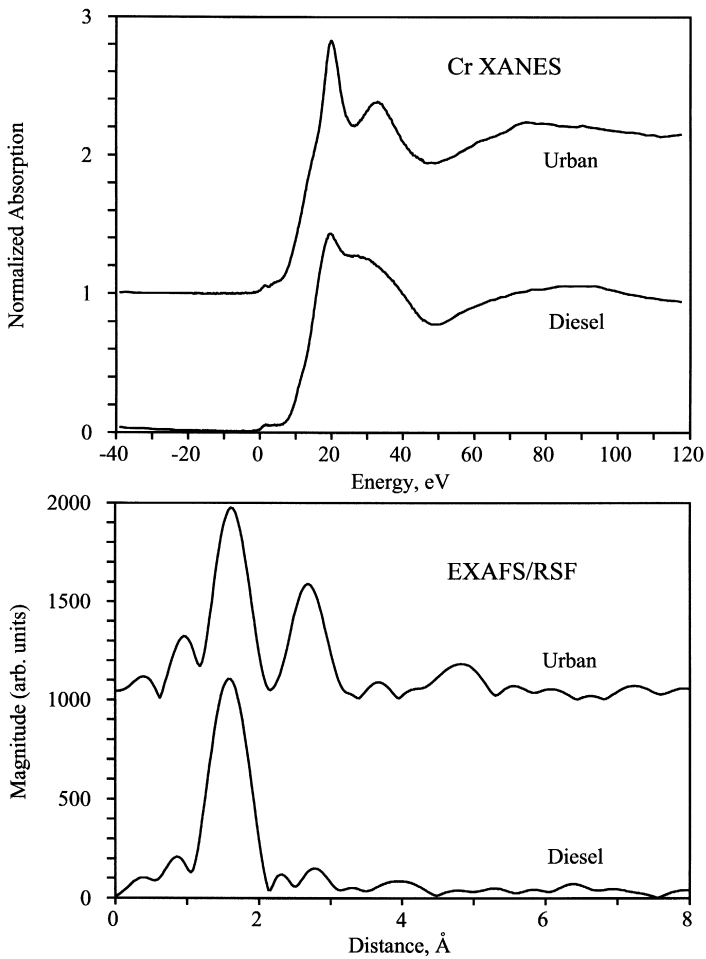

Fig. 6. Chromium XANES (top) and EXAFS/RSF (bottom) spectra of the NIST urban and diesel PM SRMs.

pre-edge peak and the vanadium XANES systematics published by Wong et al. [21], the valence state is most likely V^{4+}. The overall shape of the XANES spectrum is consistent with spectra of vanadyl compounds and V_2O_4 presented by Wong et al. [21] in which tetravalent vanadium is coordinated by oxygen anions.

3.2.4. Chromium

The concentrations of chromium in the SRMs (Table 2) were sufficient to provide not only the XANES spectra but also the RSFs derived from the EXAFS regions that are shown in Fig. 6. The XANES and RSF spectra are clearly quite different for the two samples; but the lack of a significant peak at 4.0 eV that is no more intense than the small peak at 2.0 eV in both XANES spectra shows that the oxidation state of the chromium is predominantly (> 95%), if not entirely, trivalent in both SRMs [22].

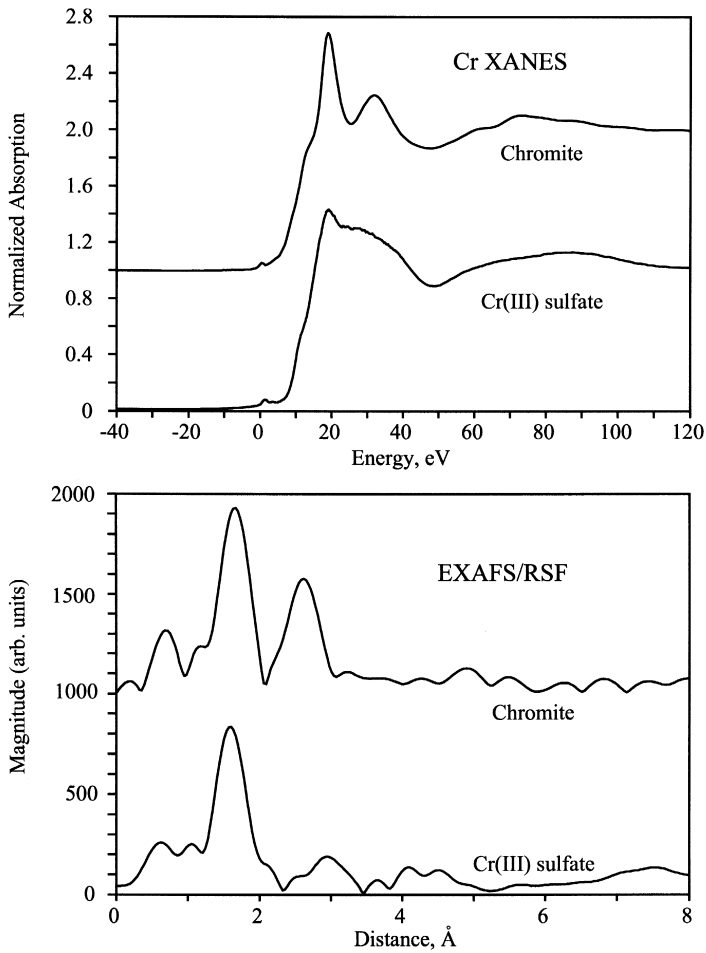

Fig. 7. Chromium XANES (top) and EXAFS/RSF (bottom) spectra of chromium in chromite ($FeCr_2O_4$) and chromium sulfate ($Cr_2(SO_4)_3 \cdot xH_2O$). Note the similarity of these spectra to those shown in Fig. 7.

Moreover, the major peak positions at about 1.6 Å in the RSFs are consistent with Cr^{3+} in six-fold coordination by oxygen anions.

The chromium XANES of the two SRMs are quite distinctive, and by comparison with a database of XAFS spectral data on chromium standards [22,23], a good match was found for the Cr XANES spectra of the urban and diesel SRMs with those for Cr in a spinel structure and a Cr^{3+} sulfate, respectively. These comparative spectra for the standards are shown in Fig. 7. It is reassuring too that the RSF spectra for the standards (also shown in Fig. 7) agree closely with the observed RSFs for the SRMs. Such distinctive chromium XANES spectra could find use as potential source signatures to aid in the recognition of individual source contributions to ambient airborne PM.

3.2.5. Manganese

The manganese XANES spectra of the two SRMs are shown in Fig. 8. The corresponding RSFs (not shown) were not of particularly good quality and were not used for the interpretation. There is a pre-edge peak in both XANES spectra at about 1–2 eV; for the diesel PM, this peak is exceedingly small, but it is somewhat more intense for the urban PM. The low energy and small intensity of such peaks suggest a relatively low oxidation state for manganese in these materials [24]. Divalent manganese is indicated as the dominant oxidation state for manganese in the diesel PM based on the very small height of the pre-edge peak and the overall shape of the XANES spectrum, which is similar to that for Mn^{2+} in aqueous solution [9,25]. However, a significant fraction of a higher oxidation state (Mn^{3+} or Mn^{4+}??) may be present in the urban PM sample. Comparison of the experimental data with published manganese XANES spectra [9,24] has not been conclusive in identifying specific Mn forms.

3.2.6. Iron

The iron speciation in the SRMs was examined by ^{57}Fe Mössbauer spectroscopy, a more definitive speciation technique for iron than XAFS spectroscopy. The iron content

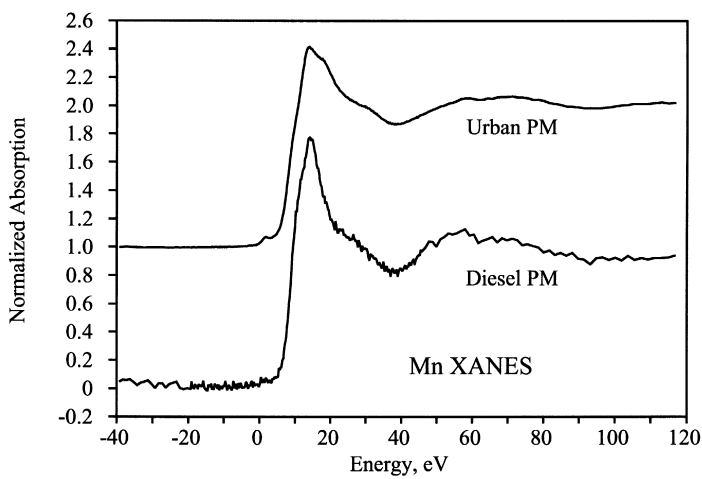

Fig. 8. Manganese XANES spectra of the NIST urban and diesel PM SRMs.

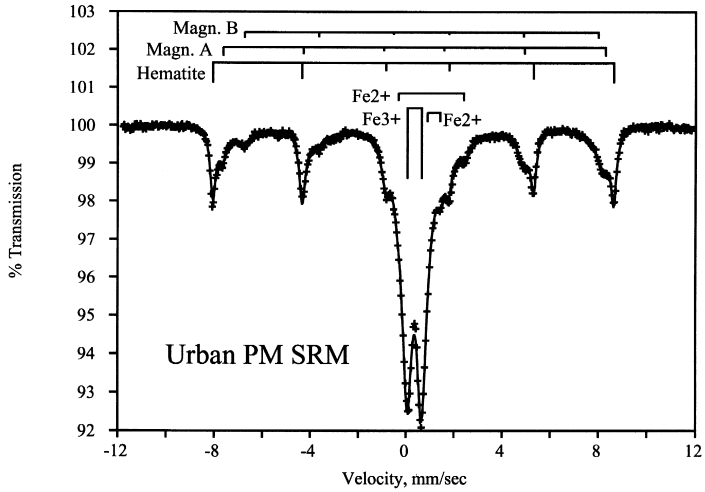

Fig. 9. Mössbauer spectrum of the NIST urban PM SRM. As indicated by the bar diagrams, the spectrum is least-squares fitted to three magnetic and three quadrupole components.

(Table 2), however, was not sufficient for a good spectrum in the case of the diesel PM and data are presented here for the urban PM only. The Mössbauer spectrum is shown in Fig. 9; it has been fit, as indicated, as the combination of three 6-line magnetic contributions and three 2-line quadrupole contributions. The results of the fitting are summarized in Table 4. The fact that one can fit the Mössbauer spectrum to six distinct components indicates that the technique is more definitive than XAFS spectroscopy. About 40% of the iron is present as the magnetic oxide species, magnetite and hematite; the remaining 60% of the iron is predominantly ferric and exists either in a clay mineral or possibly in a non-magnetic iron oxyhydroxide (FeOOH). The minor Fe^{2+} components would be more compatible with iron in a clay mineral; however, they could also be independent Fe^{2+} species. The data do not appear to be compatible with significant iron in sulfate species, as both the ferric and ferrous isomer shift values appear too low

Table 4
Results from least-squares fitting of ^{57}Fe Mössbauer spectrum for the urban PM

Fe species	Mössbauer parameters[a]			% Fe
	IS (mm/s)	QS (mm/s)	MHS (kG)	
Fe^{3+} oxide? clay?	0.36	0.60	–	51
Fe^{2+}	1.04	2.73	–	5
Fe^{2+}	1.15	0.54	–	6
Magnetite-A	0.33	–	493	12
Magnetite-B	0.63	–	456	12
Hematite	0.38	−0.10	517	15

[a]IS, QS, and MHS, are the Mössbauer parameters, isomer shift, quadrupole splitting, and magnetic hyperfine splitting, respectively.

for such species [12]. Additional Mössbauer work will be undertaken at cryogenic temperatures for more definitive assignment of the non-magnetic components.

3.2.7. Copper

Copper is fairly abundant in both SRMs (Table 2), especially the urban PM, and both samples give reasonably good quality XANES and RSF spectra (Fig. 10). Unlike for most of the elements discussed so far, the spectra arising from the two SRMs are not too dissimilar. A suite of copper XANES spectra are shown in Fig. 11 for copper metal and a variety of copper sulfides, oxides, and Cu^{2+} standard compounds. Upon comparing the XANES for the SRMs and those for the copper standards, it is clear that the copper species in the two SRMs are neither metallic nor sulfidic, but appear more like the cupric standard compounds, especially the hydrated copper sulfate, $CuSO_4 \cdot xH_2O$, shown in Fig. 11. The major peak in the RSFs of the SRMs occurs at 1.55–1.6 Å; such a

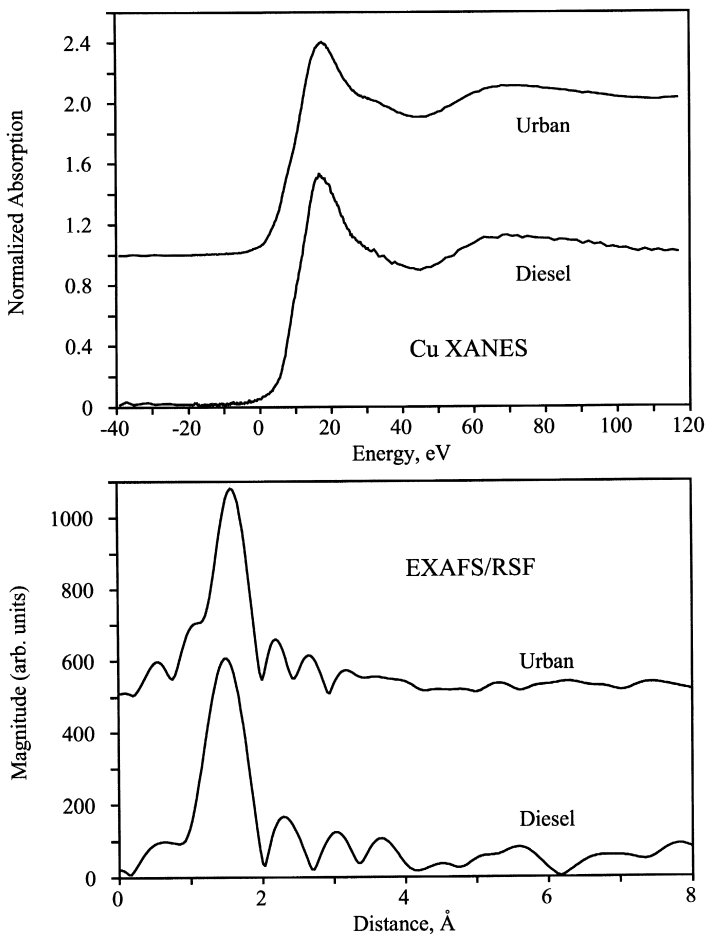

Fig. 10. Copper XANES (top) and EXAFS/RSF (bottom) spectra of the NIST urban and diesel PM SRMs.

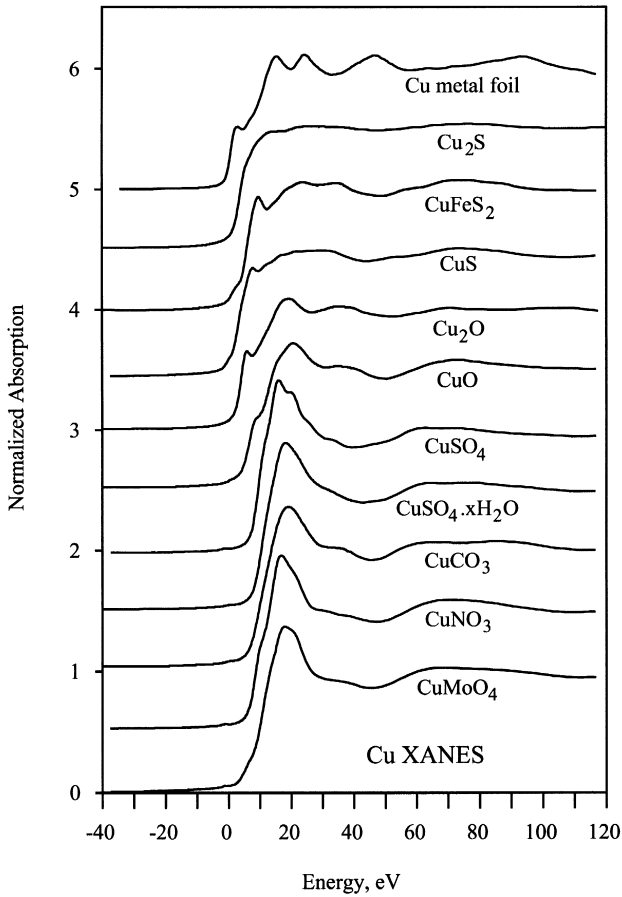

Fig. 11. Suite of copper XANES spectra for copper metal and various sulfides, oxides, and Cu^{2+} compounds.

peak position is compatible with six-fold coordinated Cu^{2+} surrounded by oxygen anions.

3.2.8. Zinc

Owing to the high concentration of zinc in the SRM samples (Table 2), well-defined zinc XANES and RSF spectra were obtained for both samples (Fig. 12). Based on the zinc XANES and RSF peak systematics discussed by Priggemeyer et al. [26], zinc in both samples is predominantly in six-fold coordination by oxygen anions. Further, the similarity of the XANES spectrum of the diesel PM to that of zinc sulfate ($ZnSO_4 \cdot 7H_2O$) suggests that the zinc occurs as a hydrated sulfate species in the diesel PM. The Zn spectrum of the urban PM sample is similar to that of the diesel SRM, but there are significant minor differences that suggest the occurrence of zinc in additional forms. The RSFs of both SRM samples are compatible with zinc in six-fold coordination by oxygen anions.

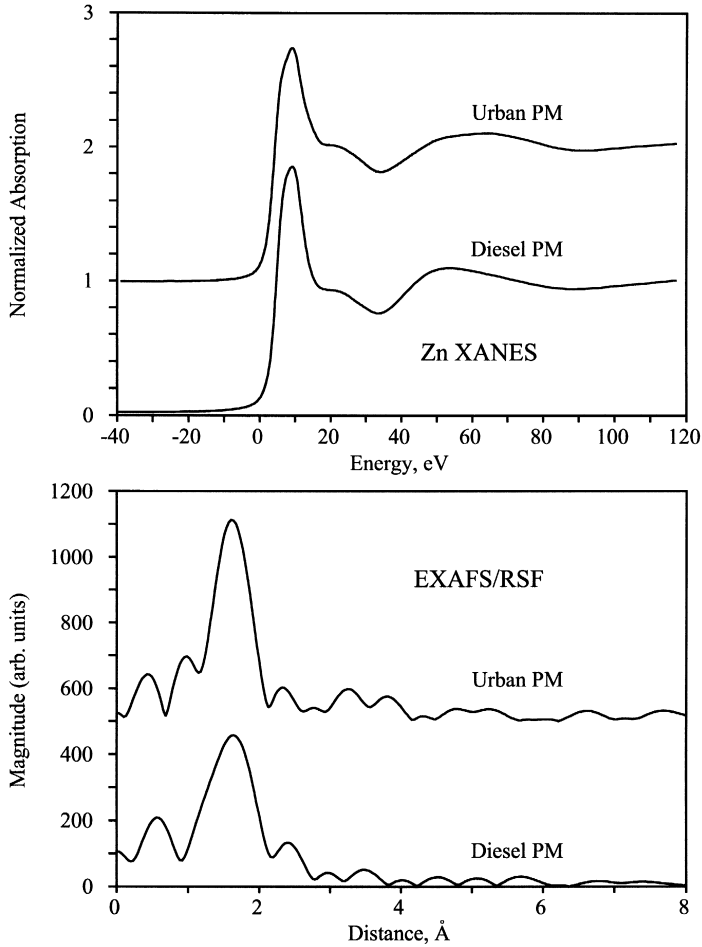

Fig. 12. Zinc XANES (top) and EXAFS/RSF (bottom) spectra of the NIST urban and diesel PM SRMs.

3.2.9. Arsenic

The arsenic contents of the SRM samples are relatively low (Table 2); however, reasonable arsenic XANES spectra (Fig. 13) were obtained for both samples, and a RSF was obtained for the urban PM (not shown). Based on the position of the major peak in the XANES spectra [22,27], the dominant oxidation state of arsenic in both samples is As(V), as occurs in arsenate [AsO_4^{3-}] anion species. A single peak was observed in the RSF obtained from the urban PM; the occurrence of this peak at 1.33 ± 0.03 Å is also compatible with arsenate complexes [22,27].

As can be seen in Fig. 13a, the XANES spectra are asymmetric on the low-energy side of the peak. By means of a least-squares fitting program, a small peak at about 0 eV is indicated to be responsible for this asymmetry (Fig. 13b). This peak arises from a small fraction ($10 \pm 5\%$) of the arsenic present as As(III). This observation is significant

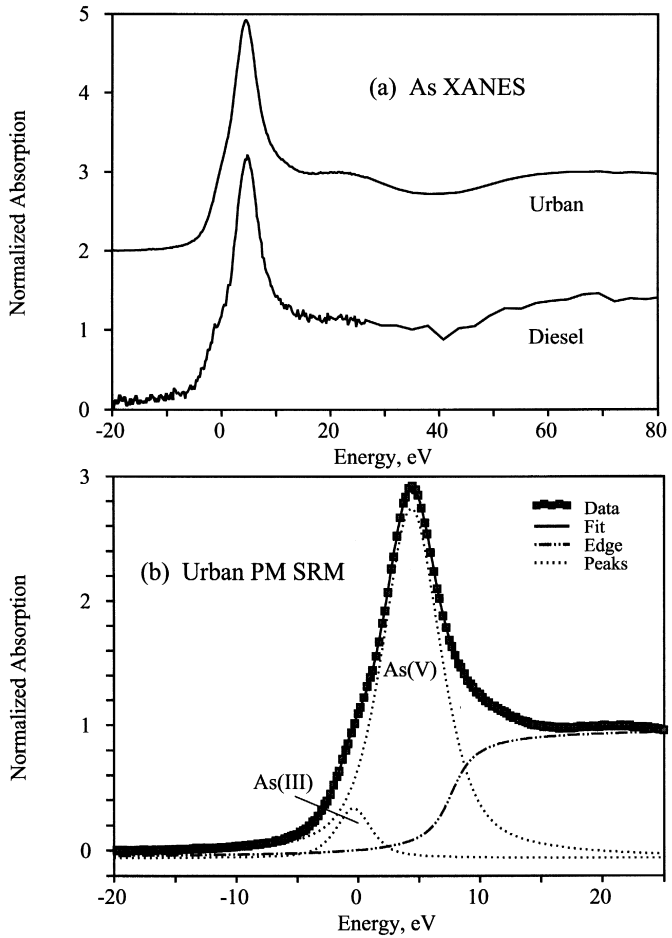

Fig. 13. (a) Arsenic XANES spectra of the NIST urban and diesel PM SRMs. (b) Least-squares fitted arsenic XANES spectrum for the urban PM indicating the minor presence of an As(III) species.

because the As(III) oxidation state is known to be many times more toxic than the As(V) oxidation state [28,29]. Hence, this small fraction of As(III) effectively makes the arsenic in these two samples considerably more toxic than it would have been had all of the arsenic been present as As(V).

3.2.10. Cadmium

Data were also collected for cadmium in both SRMs and the XANES spectra and are shown in Fig. 14. The spectra appear similar, but this is not unexpected because the XANES spectra of cadmium compounds do not vary much (Fig. 15). It is therefore difficult to make significant conclusions from the cadmium XAFS data alone. However, it can be noted that the shape of the cadmium XANES spectra for the SRMs appears more consistent with Cd in coordination by oxygen, as in cadmium sulfate or cadmium

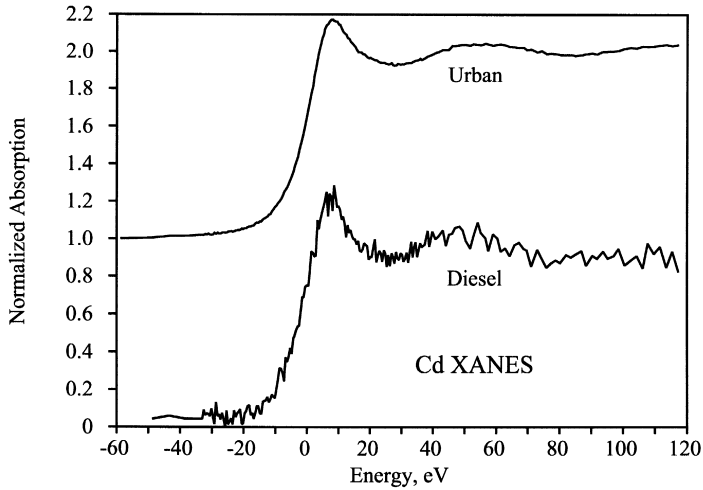

Fig. 14. Cadmium XANES spectra of the NIST urban and diesel PM SRMs.

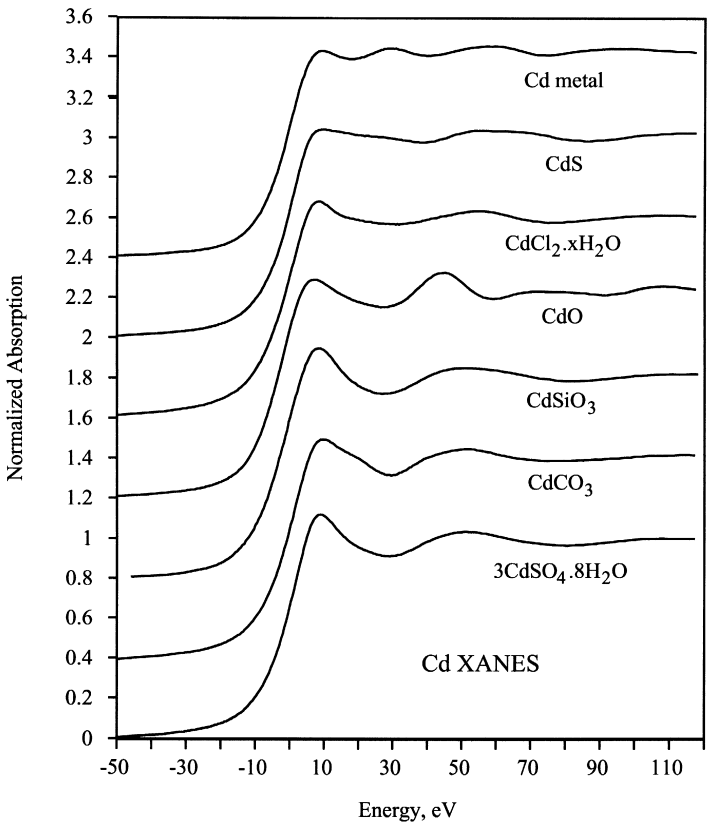

Fig. 15. Suite of cadmium XANES spectra for cadmium metal, and various cadmium compounds.

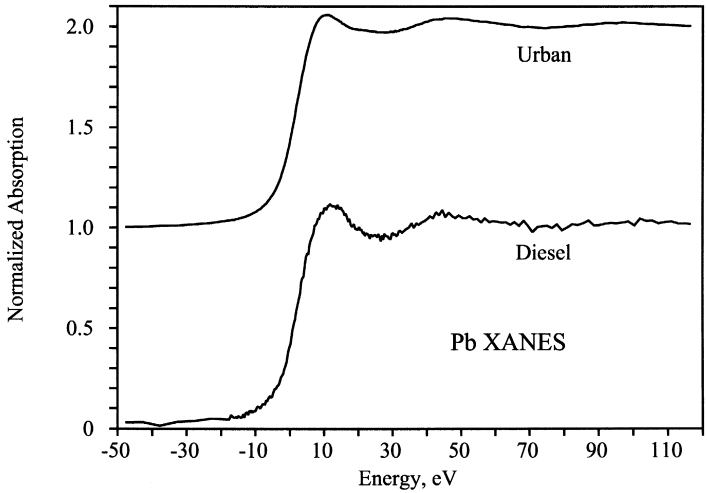

Fig. 16. Lead L_{III}-edge XANES spectra of the NIST urban and diesel PM SRMs.

silicate, and the RSF data for the urban PM (not shown) is compatible with a long Cd—O bond. Hence, although the data indicate that Cd is present in an environment of oxygen anions, the actual speciation of cadmium in the SRMs remains ambiguous.

3.2.11. Lead

Data were also collected at the L_{III} absorption edge for lead in both SRMs and the XANES spectra and are shown in Fig. 16. The spectra show some minor differences that suggest that the lead forms in the two samples may be different. But like cadmium, lead compounds do not show much variation and it is difficult to make strong conclusions based on relatively minor differences. Hence, the lead speciation is also ambiguous.

4. Conclusions

The speciation of elements in NIST SRMs 1648 and 1650, urban and diesel PM samples, has been investigated by XAFS and Mössbauer spectroscopies. Complementary data from PIXE spectroscopy on elemental compositions have also been obtained. A number of significant observations on element speciation in these PM SRMs have been made; these are summarized in Table 5 on an element-by-element basis.

In virtually all cases where an element can be found in more than one oxidation state, the XAFS and Mössbauer spectroscopic techniques provide direct information about the relative abundance of the oxidation states, even for elements present in concentrations less than 10 ppm or below their detection limits for PIXE spectroscopy. We have been able to estimate, in some cases, quantitatively, the relative fractions of different oxidation states of sulfur, vanadium, chromium, iron, and arsenic in the two NIST SRMs. Often, it is the oxidation state that is the most important parameter in determin-

Table 5
Summary of speciation information obtained on NIST urban and diesel PM SRMs

Element	SRM	Observation on speciation
Sulfur	Urban	predominantly sulfate; $<5\%$ S as organosulfur
	Diesel	predominantly bisulfate; 10% S as organosulfur (thiophene?)
Chlorine	Urban	mixture of inorganic and organic Cl forms
	Diesel	predominantly organochlorine forms
Vanadium	Urban	predominantly V^{4+} in oxygen coordination
	Diesel	significant edge not detected
Chromium	Urban	Cr^{3+} in spinel $[(Fe,Mg)(Al,Fe,Cr)_2O_4]$
	Diesel	Cr^{3+} in sulfate $[(Cr_2(SO_4)_3 \cdot xH_2O)]$
Manganese	Urban	mixture of low oxidation states (Mn^{2+}, Mn^{3+}?, Mn^{4+}?) matrix unknown
	Diesel	predominantly Mn^{2+} in coordination by H_2O?
Iron	Urban	predominantly Fe^{3+} ($>80\%$), minor Fe^{2+} ($<20\%$) matrix consists of magnetic oxides and possibly clay
	Diesel	no data
Copper	Urban	Cu^{2+} sulfate and minor other forms?
	Diesel	Cu^{2+} sulfate $[CuSO_4 \cdot xH_2O]$
Zinc	Urban	Zn sulfate and other zinc forms
	Diesel	Zn sulfate, $[ZnSO_4 \cdot xH_2O]$
Arsenic	Urban	90% as As^{5+} arsenate anion; 10% as As^{3+}
	Diesel	90% as As^{5+} arsenate anion; 10% as As^{3+}
Bromine	Urban	similar to chlorine?
	Diesel	similar to chlorine?
Cadmium	Urban	Cd in oxygen coordination (sulfate?, silicate?)
	Diesel	Cd in oxygen coordination??
Lead	Urban	Pb^{2+} in oxygen coordination
	Diesel	Pb^{2+} in oxygen coordination??

ing both the toxicity of an element and its aqueous solubility and, as is well known, both of these factors are important in how an element in airborne PM interacts with the human body via the pulmonary system. For chromium and arsenic, for which the actual oxidation state is very critical to the overall toxicity of the element, there was no evidence for the Cr(VI) oxidation state, and, although arsenic was shown to be present predominantly in the less toxic As(V) oxidation state, the observed small As(III) fraction may be a significant contribution to the overall toxicity of arsenic.

In addition, the spectroscopic techniques provide an indication of how the elements occur in the NIST urban and diesel PM SRMs. For these materials, all of the metallic elements investigated appear to occur in oxidized forms; there was no evidence for any metallic or sulfidic occurrences of these elements. Further, most of the metallic elements appeared to occur principally as sulfates in the diesel PM; whereas, the occurrences in the urban PM were more varied and included oxide and perhaps aluminosilicate (clay mineral?) occurrences, in addition to sulfate. There was an evidence for organosulfur (thiophene?) and organohalide occurrences. A small fraction of the sulfur and perhaps major fractions of the halogen elements, chlorine and bromine, appear to be associated with the carbonaceous materials in these SRMs, especially the diesel PM SRM. Arsenic, a semi-metallic element, occurred principally as arsenate and was therefore different

from both the true metallic elements and non-metallic elements investigated. Possibly, such arsenate occurrences are associated with the abundant sulfate occurrences, as often occurs in the mineral world.

Finally, we must make note of the highly specific information obtained from chromium XAFS spectroscopy. Using this technique, we have been able to identify successfully specific forms of occurrence of this element in both SRMs. Indeed, the recognition of the chromite spinel phase in the urban PM raises some very interesting questions concerning how such a highly refractory chromium-bearing phase could be so prevalent in an urban environment, but such speculations are outside the scope of this paper. In a large part, this success is due to having an extensive database of standard spectra available for chromium, and we would anticipate similar success with other elements, once comparable databases are established. However, it is clear that the XAFS data for this element, and perhaps others as well, have potential for use as a characteristic signature for specific sources of PM. Similarly, the Mössbauer spectrum for iron could also find use as a possible source signature.

The XAFS spectroscopic technique has a significant potential for directly and nondestructively speciating critical elements in the complex materials encountered in ambient PM samples and PM source materials and for helping provide answers to important questions regarding the toxicity and source apportionment of such materials. In addition, the technique provides complementary information to that obtained by other types of analyses that can be done on PM [2,30]. However, a much wider variety of PM samples needs to be examined, and more data obtained with the XAFS technique before its full potential will be realized for characterization of such complex materials.

Acknowledgements

We acknowledge the assistance of Dr. Fulong Lu, formerly of the University of Kentucky, and the SSRL Biotechnology Group for help with the XAFS data collection, and Element Analysis, Lexington, KY, for providing PIXE analyses of the NIST urban and diesel PM SRMs. We also acknowledge the US Department of Energy for its support of the operation of synchrotron facilities in the USA.

References

[1] US EPA, National ambient air quality standards for particulate matter — Final rule. Federal Register 62 (1997) 38651–38760, (July 18).
[2] $PM_{2.5}$: A Fine Particle Standard, J. Chow, P. Koutrakis (Eds.), Proc. Specialty Conf., Long Beach, CA, VIP-81 Vols. I and II Air and Waste Management Association, Pittsburgh, PA, 1998.
[3] S.A. Benson, J.H. Pavlish, T.D. Brown, W.G. Stelz (Eds.), Proceedings, Conference on Air Quality, McLean, VA, Energy and Environmental Research Center, Grand Forks, ND, 1998.
[4] Amendments to the Clean Air Act, US Public Law 101-549, US Gov. Printing Office, 1990, 314 pp.
[5] F.E. Huggins, N. Shah, G.P. Huffman, J. David Robertson, Fuel Proc. Technol. (2000) in press.
[6] F.W. Lytle, R.B. Greegor, D.R. Sandstrom, E.C. Marques, J. Wong, C.L. Spiro, G.P. Huffman, F.E. Huggins, Nucl. Instrum. Methods 226 (1984) 542–548.

[7] S.P. Cramer, O. Tench, N. Yocum, G.N. George, Nucl. Instrum. Methods A 266 (1988) 586–591.
[8] E.A. Stern, S.M. Heald, Rev. Sci. Instrum. 50 (1979) 1579–1582.
[9] G.E. Brown Jr., G. Calas, G.A. Waychunas, J. Petiau, in: F.C. Hawthorne (Eds.), Spectroscopic Methods in Mineralogy and Geology, Rev. Miner. Vol. 18, Mineralogical Society of America, Washington, DC, 1988, pp. 431–512, Chap. 11.
[10] P.A. Lee, P.H. Citrin, P. Eisenberger, B.M. Kincaid, Rev. Mod. Phys. 53 (1981) 769–808.
[11] D.C. Koningsberger, R. Prins, X-ray Absorption. Principles, Applications, Techniques of EXAFS, SEXAFS, and XANES, Wiley, New York, 1988.
[12] F.E. Huggins, G.P. Huffman, in: C. Karr Jr. (Ed.), Analytical Methods for Coal and Coal Products Vol. III Academic Press, New York, NY, 1979, pp. 371–423, Chap. 50.
[13] A.S. Wong, J.D. Robertson, J. Coal Qual. 12 (1993) 146–150.
[14] J.A. Maxwell, J.L. Campbell, W.J. Teesdale, Nucl. Instrum. Methods B 43 (1989) 218–230.
[15] National Institute of Standards and Technology, Certificate of Analysis, Standard Reference Material 1648, Urban Particulate Matter, August 30, 1991, 5 pp.
[16] National Institute of Standards and Technology, Certificate of Analysis, Standard Reference Material 1650, Diesel Particulate Matter, December 12, 1991, 7 pp.
[17] G.P. Huffman, S. Mitra, F.E. Huggins, N. Shah, Energy Fuels 5 (1991) 574–581.
[18] M.M. Taghiei, F.E. Huggins, N. Shah, G.P. Huffman, Energy Fuels 6 (1992) 293–300.
[19] F.E. Huggins, S.V. Vaidya, N. Shah, G.P. Huffman, Fuel Process. Technol. 35 (1993) 233–257.
[20] F.E. Huggins, G.P. Huffman, Fuel 74 (1995) 556–569.
[21] J. Wong, F.W. Lytle, R.P. Messmer, D.H. Maylotte, Phys. Rev. B 30 (1984) 5596–5610.
[22] F.E. Huggins, N. Shah, J. Zhao, F. Lu, G.P. Huffman, Energy Fuels 7 (1993) 482–489.
[23] F.E. Huggins, M. Najih, G.P. Huffman, Fuel (Special Issue, 1997 International Ash Utilization Symposium) 78 (1999) 233–242.
[24] A. Manceau, A.I. Gorshkov, V.I. Drits, Am. Mineral. 77 (1992) 1133–1143.
[25] J. Garcia, A. Bianconi, M. Benfato, C.R. Natoli, J. Phys. 47 (C8) (1986) 49–54.
[26] S. Priggemeyer, P. Eggers-Borkenstein, F. Ahlers, G. Henkel, M. Körner, H. Witzel, H.-F. Nolting, C. Hermes, B. Krebs, Inorg. Chem. 34 (1995) 1445–1454.
[27] G.P. Huffman, F.E. Huggins, N. Shah, J. Zhao, Fuel. Process. Technol. 39 (1994) 47–62.
[28] N.W. Tietz (Ed.), Clinical Guide to Laboratory Tests, 2nd edn., Saunders, Philadelphia, PA, 1990.
[29] N.C. Korte, Q. Fernando, Crit. Rev. Environ. Contr. 21 (1991) 1–39.
[30] L.L. Sloss, Sampling and Analysis of PM10/PM2.5, Report CCC/09, IEA Coal Research, London, 998, 38 pp.